JMEPEG (2022) 31:3200–3207
https://doi.org/10.1007/s11665-021-06447-z

1059-9495/$19.00

TECHNICAL ARTICLE

Structure and Tribo-Mechanical Properties of MoS_x:N:Mo Thin Films Synthesized by Reactive dcMS/HiPIMS

Wolfgang Tillmann, Alexandra Wittig, Dominic Stangier, Carl-Arne Thomann, Jörg Debus, Daniel Aurich, and Andreas Brümmer

Submitted: 14 April 2021 / Revised: 14 September 2021 / Accepted: 26 September 2021 / Published online: 14 December 2021

Modifying MoS_2 thin films by additional elements shows great potential in order to adjust the property profile and to meet the increasing requirements regarding high wear resistance and low friction properties of industrial components. Within that context, MoS_x:N:Mo thin films were deposited by a reactive hybrid dcMS/HiPIMS process. By systematically increasing the Mo target cathode power, an investigation of the structural and the mechanical properties was conducted to understand the evolution of the tribological behavior. A low Mo target cathode power of 1 kW is related to the formation of the preferential (002) MoS_2 basal-plane and thus a low friction with $\mu = 0.2$. With an increasing amount of Mo, the film loses its solid lubricant MoS_2 properties and a nitride constitution of the thin film is developing due to the formation of crystalline Mo and MoN phases. Related to this transformation, the hardness and elastic modulus are increased, but the adhesion and the tribological properties are impaired. The film loses its plasticity and the generated film material is directly removed from the contact area during the sliding contact.

Keywords Element modification, Friction behavior, MoS_x:Mo:N, Reactive dcMS/HiPIMS

1. Introduction

Synthesizing thin films by PVD technology is a well-established method to modify the surface and thus the functionality of industrial components (Ref 1). Whereas in lubricated machining operations, thin films with a high hardness and wear resistance, as TiN and CrN, are required; in dry machining or tribological applications, thin films are demanded, which have a lubricating nature themselves, as MoS_2 and WS_2 (Ref 2). The lubricating properties of MoS_2 are caused by a lamellar structure, enabling a low shear strength (Ref 3) and the ability of forming a transfer film (Ref 4). However, the properties are impaired in humid environments due to the adsorption and diffusion of water molecules (Ref 5). In addition, the low hardness and elastic modulus are related to an insufficient load-bearing capacity (Ref 6).

To reduce the sensitivity of the tribological properties on humidity and to improve the mechanical properties, the addition of elements as Ti (Ref 7, 8) or N_2 (Ref 9, 10) into MoS_2 as well as the incorporation of MoS_2 into a hard ceramic matrix, as TiN (Ref 11-13), TiSiN (Ref 14, 15) CrN (Ref 16, 17), CrMoN (Ref 18), or CrAlN (Ref 19) exhibits great potential. Nevertheless, the structure and the mechanisms affecting the performance of the thin films deviate with respect to the chemical composition, especially the ratio between the doping element/ceramic matrix and the lubricating MoS_2 phase. Within that context, previous examinations either consider the effect of doping metallic/non-metallic elements into MoS_2 or the influence of adding MoS_2 to a nitride matrix. The impact of co-incorporating metallic and non-metallic elements on the properties of MoS_2 thin films, in particular with regard to their ability of forming new phases, is not yet investigated so far. Therefore, MoS_x:N:Mo thin films were deposited by a reactive dcMS/HiPIMS process. Subsequently, the effect of an increasing Mo cathode power on the structure and the tribo-mechanical properties of the thin films was analyzed.

Wolfgang Tillmann, Alexandra Wittig, and **Dominic Stangier**, Institute of Materials Engineering, TU Dortmund University, Leonhard-Euler-Straße 2, 44227 Dortmund, Germany; **Carl-Arne Thomann** and **Jörg Debus**, Experimental Physics 2, TU Dortmund University, Otto-Hahn-Straße 4a, 44227 Dortmund, Germany; and **Daniel Aurich** and **Andreas Brümmer**, Chair of Fluidics, TU Dortmund University, Leonhard-Euler-Straße 5, 44227 Dortmund, Germany. Contact e-mails: wolfgang.tillmann@tu-dortmund.de, alexandra.wittig@tu-dortmund.de, dominic.stangier@tu-dortmund.de, carlarne.thomann@tu-dortmund.de, joerg.debus@tu-dortmund.de, daniel.aurich@tu-dortmund.de, and andreas.bruemmer@tu-dortmund.de.

2. Experimental

2.1 Film Deposition

The deposition process of the MoS_x:N:Mo thin films was carried out in an industrial sputtering device CC800/Custom (CemeCon AG, Germany). As substrate material the steel 16MnCr5 with a hardness of (10.0 ± 0.5) GPa was selected. Grinding and polishing processes were applied to obtain a roughness of $R_a = (3.1 \pm 0.6)$ nm. Prior to the deposition process, a heating and etching sequence was carried out in the sputtering device. Therefore, the temperature was increased up to approximately 200° and a noble gas etching process with Ar ions at a bias-voltage of -650 V was conducted. To synthesize the MoS_x:N:Mo films, two MoS_2 targets (purity 99.95%) and two Mo targets (purity 99.95%) were used. Whereas the MoS_2 targets were sputtered in HiPIMS mode, for

the Mo targets a dc power supply was selected. As pulse parameters a frequency of 1000 Hz and a pulse duration of 200 μs were chosen at a heating power of 1000 W and a bias-voltage of -100 V. The parameters were selected according to (Ref 20). The nitrogen-controlled working pressure was kept constant at 50 sccm, using argon as working gas with a pressure of 400 mPa. In order to modify the chemical composition of the films, three different Mo target cathode power (cp_{Mo}) levels: 1, 2 and 3 kW were used.

2.2 Film Characterization

The chemical composition, the morphology and the topography of the thin films were investigated by means of scanning electron microscopy (SEM), using a JSM-7001F (JEOL, Japan) with an acceleration voltage of 20 kV and a probe current of 15 μA. The chemical composition was determined by energy dispersive x-ray spectroscopy (EDS) using an INCAx-act detector (Oxford Instruments, United Kingdom). Furthermore, the crystallographic orientation was analyzed using an Advanced D8 (Bruker AXS, United States of America) diffractometer. The measurements were conducted in a 2 Θ-angle range from 10 to 100° with a step size of $\Delta\theta = 0.035°$ and an exposure time of 1 s. In order to examine the hardness H and the elastic modulus E, nanoindentation tests were performed with the nanoindenter G200 (Agilent, USA). In total, 49 indents per sample were conducted with a Berkovich diamond tip in the continuous stiffness mode (Ref 21, 22). The mechanical properties were measured in a depth not exceeding 10% of the film thickness to prevent an influence of the substrate. A Poisson ratio of $\nu = 0.2$ was assumed (Ref 23). Besides, the effective Young´s modulus was calculated from the equation $E^* = E/(1-\nu^2)$ in order to determine the H/E* ratio as plasticity index related to the elastic strain failure and the H^3/E^{*2} ratio related to the resistance to plastic deformation. The adhesion was evaluated by the Rockwell C indentation test according to the German guideline VDI 3198. A load of 1 kN was applied on the coated substrates. To determine the coefficients of friction, a tribometer (CSM Instruments SA, Switzerland) in ball-on-disc configuration was used. As test parameters a normal load of 5 N with a sliding velocity of 0.4 m/s and 5000 rotations were selected in ambient air with a relative humidity of 40%. The wear coefficients, as amount of the removed film material, were evaluated by a 3D profilometer (Alicona, Austria). In addition, SEM images from the wear track were taken and 3D-models were generated with the software Leica Maps 8 (Leica, Germany).

3. Results and Discussion

3.1 Structural Properties

The chemical composition of the thin films is illustrated in Table 1.

It can be seen that an increasing Mo target cathode power directly results in a higher Mo content as well as a reduction of the S content in the thin films. At the same time, the N_2 content increases. All films are characterized by a sub-stoichiometric character, which is a typical feature of sputtered MoS_2 thin films. This effect is ascribed to a loss of S during the transport through the plasma (Ref 24) and a preferential re-sputtering of S during the film growth process (Ref 25, 26) caused by the lower atomic mass of S compared to Mo. Both mechanisms are suggested to be more pronounced in HiPIMS due to the related increased plasma density and the high kinetic energy of the sputtered particles (Ref 27). By using additional Mo targets, an enhanced amount of Mo is sputtered and the S/Mo ratio is therefore shifted to lower values. Although the N_2 flow rate has been kept constant for all deposition processes, the N_2 amount in the films increased. This effect is attributed to the formation of MoN, which will be discussed below.

For the examination of the crystallographic orientation, x-ray diffraction measurements were conducted (see Fig. 1). The thin film only synthesized with MoS_2 targets shows the (100) and (110) reflexes belonging to hexagonal MoS_2. Due to the use of additional Mo targets with a cathode power of 1 kW, these both reflexes vanish and the film exhibits a pronounced (002) reflex. By further increasing the Mo cathode power, reflexes related to crystalline Mo and MoN can be identified. The film synthesized without additional Mo targets can be characterized as edge-plane oriented, since the (100) reflex is most pronounced (Ref 28, 29). By applying a Mo target cathode power of 1 kW, a shift from (100) edge-plane to (200) basal-plane oriented occurs. Similar effects are achieved by depositing a multilayer structure, where a periodic deposition of metal layers interrupts the crystallite growth. The metal layers

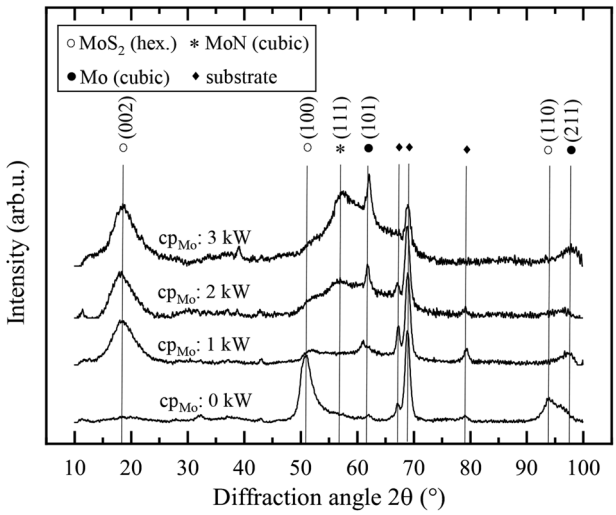

Fig. 1 X-ray diffractograms of the MoS_x:N:Mo thin films

Table 1 Chemical composition of the MoS_x:N:Mo thin films

cp_{Mo}/kW	Mo content/at.%	S content/at.%	N content/at.%	S/Mo ratio
0	31.2 ± 0.2	47.7 ± 2.0	21.2 ± 1.8	1.53
1	34.9 ± 1.7	35.9 ± 1.2	29.3 ± 2.7	1.02
2	36.7 ± 0.7	27.7 ± 0.5	35.5 ± 0.7	0.75
3	37.7 ± 0.1	24.2 ± 0.5	38.1 ± 0.4	0.64

act as nucleation barrier and cause a basal-plane growth, since on each layer a new growth process starts, which is typical determined by basal-planes (Ref 30-33). Although the investigated MoS_x:N:Mo film is not deposited in a multilayer structure, the manner in which it is synthesized leads to the assumption that a similar mechanism occurs. The substrates are rotated between the MoS_2 and Mo targets, and thus, the film growth is periodically interrupted. Although N_2 is introduced during the deposition process, no Bragg reflexes related to MoN are identified for a low Mo cathode power. This is attributed to the fact that MoS_2 is chemically stable in a mixed Ar/N_2 atmosphere during the reactive sputtering process (Ref 9). This is based on a higher affinity of Mo to S compared to Mo to N_2 and the related preferred formation of MoS_2, as shown for WS_2 by Nossa et al. (Ref 34). Therefore, MoN is hardly formed due to a reactive sputtering of only MoS_2 targets, respectively a low Mo target cathode power. Since no new crystalline phases are formed, it is suggested that Mo acts as a doping element and is incorporated in the spaces between the S planes or makes junctions between the MoS_2 lattice as reported for Ti (Ref 35, 36). This assumption is supported by the shift of the (002) reflex to lower 2θ-angles compared to pure MoS_2. This shift can be traced back to an expansion of the basal-planes caused by the lattice distortion related the incorporated elements (Ref 28), which also leads to an increased hardness as discussed later. In addition, the incorporation of N_2 contributes to this effect. N_2 is characterized by a lower electronegativity compared to S. Due to the reduced electron density, a compression of the lattice in direction of the basal-planes and an expansion in direction of the edge-planes occurs (Ref 9). Above a Mo cathode power of 2 kW, the amount of Mo in the films is sufficient to from crystalline Mo and MoN phases. This gives also an explanation for the increasing N_2 content with an increasing Mo target cathode power. Nevertheless, the presence of the (002) MoS_2 basal-plane leads to the suggestion that S and Mo are still incorporated as compound instead of elemental Mo and S at the grain boundaries as it was also assumed by Gangopadhyay et al. for TiN- MoS_2 films (Ref 12).

In order to examine the morphology and the topography of the thin films, SEM images are taken and illustrated in Fig. 2. The film deposited without additional Mo targets is characterized by densely packed and v-shaped columns over the whole film thickness. By sputtering Mo targets with a cathode power of 1 kW, a densification of the microstructure occurs. A further increasing Mo cathode power leads to the development of narrow columns in growth direction. Furthermore, all films exhibit a cauliflower-like topography with agglomerated grains. The v-shaped columnar structure, as identified for the film deposited without Mo targets, was also seen in a previous investigation (Ref 37). It results from adatoms diffusing between the adjacent grains due to a high adatom mobility (Ref 38) and the growth competition taking place between the differently oriented crystals (Ref 39). Since the surface energy of the (100) edge-plane is higher compared to the (002) basal-plane (Ref 40), the adatom mobility leads to a (100) edge-plane orientation of the films as seen in the XRD spectra. By applying a low cathode power to the Mo targets, the film loses the columnar character and a densification occurs. A further increased Mo cathode power is related to a columnar structure and indicates the crystalline character due to the formation of crystalline Mo and MoN (Table 1).

3.2 Mechanical Properties

To investigate the mechanical properties, the hardness and the elastic modulus were determined (see Fig. 3 a). The values of the hardness and the elastic modulus are enhanced by an increasing Mo target cathode power from (0.9 ± 0.1) GPa and

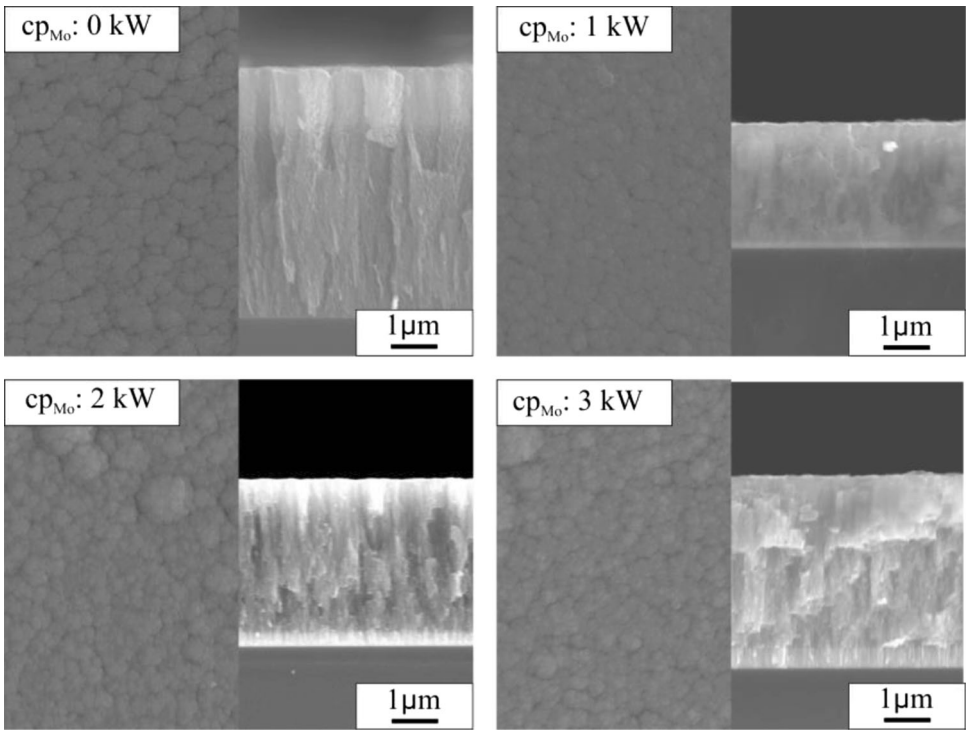

Fig. 2 SEM images of the morphology and topography of the MoS_x:N:Mo thin films

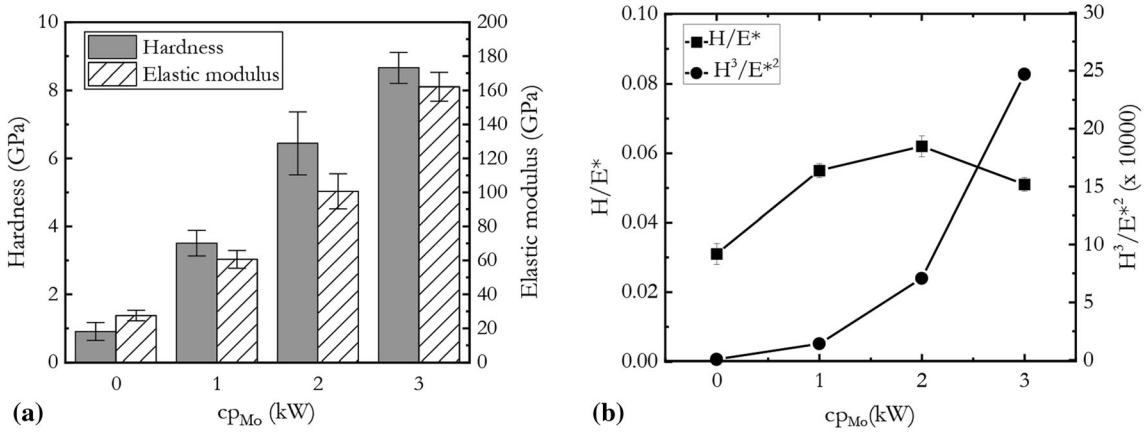

Fig. 3 (a) Hardness and elastic modulus and (b) H/E* and H^3/E^{*2} of the MoS_x:N:Mo thin films

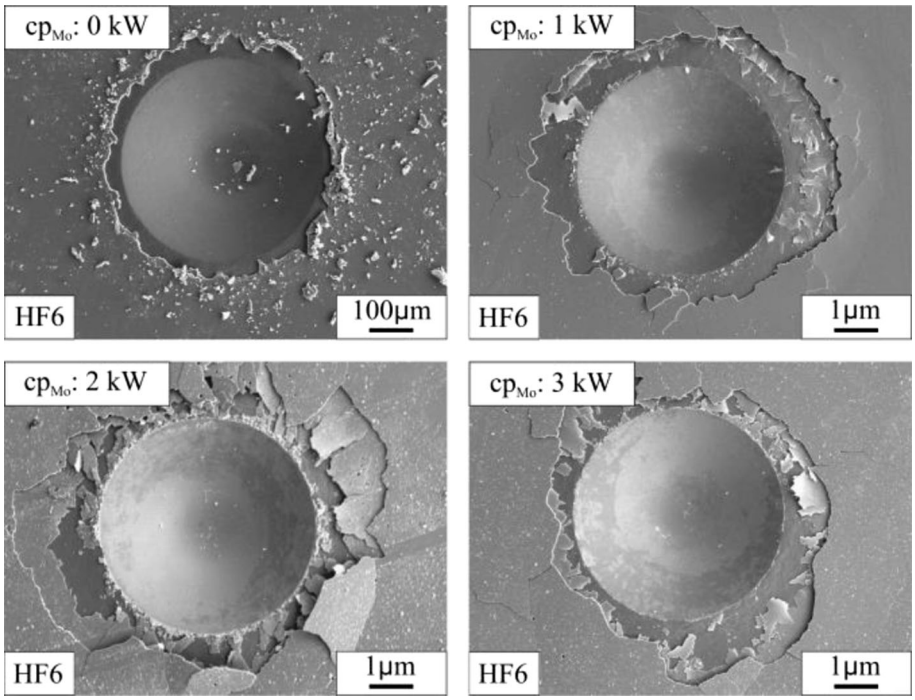

Fig. 4 SEM images of the Rockwell indents of the MoS_x:N:Mo thin films

(27.6 ± 2.1) GPa for no additional Mo targets up to (8.66 ± 0.7) GPa and (162.1 ± 9.3) GPa for a cathode power of 3 kW. The film deposited without additional Mo targets shows the lowest hardness and the elastic modulus. Thus, the incorporated N_2 amount does not affect the mechanical properties and the film exhibits similar characteristics to sputtered MoS_2 and MoS_2:N films (Ref 41). This behavior is also reflected in the chemical composition and the crystallographic orientation. For a cathode power of 1 kW, the additional incorporated Mo is related to a hardness enhancement, which is caused by a solid solution hardening effect due to the distortion of the MoS_2 lattice by the doping element, which was also seen due to the shift of the MoS_2 reflexes in the diffractogram (Ref 42, 43). By further increasing the Mo target cathode power, the formation of the hard MoN phase besides the soft MoS_2 phase is responsible for the increased hardness (Ref 44). Furthermore, it is to note that the synthesized films do not improve the hardness compared to the substrate, but the hardness is increased compared to the not-modified film. In addition, H/E* and H^3/E^{*2} as plasticity and resistance to plastic deformation are shown in Fig. 3 b. Both ratios increase with an increasing Mo target cathode power. For all films deposited with additional Mo targets, the H/E* ratio is at a similar level.

Moreover, the adhesion of the films was evaluated by Rockwell indents (see Fig. 4). Considering the SEM images of the Rockwell indents, all films are marked by an insufficient adhesion reflected in film delaminations around the indent. Therefore, all films are classified in adhesion class HF6. However, there are differences regarding the appearance and the degree of the spalling. For a Mo target cathode power of 1 kW, the area of the removed film material increased compared to 0 kW. At 2 kW, the area around the indent is characterized by cracks and detached material. Due to the additional Mo, the adhesion is further impaired, since the area

of the removed film material is increased. For a low Mo target cathode power, the adhesion is sufficient due to the low hardness. Similar results are obtained in a previous investigation regarding the incorporation of an increasing amount of N_2 (Ref 41). Although the hardness and the elastic modulus as well as the H/E* and H^3/E^{*2} are enhanced with an increasing Mo target cathode power, the adhesion is impaired. Due to the formation of the MoN phase, the residual stress within the films is increased, which is responsible for the higher hardness, but impairs the adhesion at the same time. This trend reflects the changes regarding the characteristics of the films from a solid lubricant to a nitride based film, which is directly linked to the tribological properties discussed in the next section.

3.3 Tribological Properties

To analyze the tribological properties of the synthesized thin films, the coefficients of friction against 100Cr6 counterparts and the wear coefficients were determined. The corresponding values are illustrated in Fig. 5. In addition, the development of the friction over the amount of rotations is given in Fig. 6 and SEM images as well as 3D-models of the wear tracks are shown in Fig. 7. The film deposited without Mo targets and the film synthesized with a Mo target cathode power of 1 kW exhibit the lowest coefficients of friction with values about 0.2. The coefficient of friction develops homogeneously over the amount of rotations. By further increasing the Mo cathode power to 2 and 3 kW, the friction increases directly after few rotations up to 1 and then settles to a value between 0.7 and 0.8. The wear coefficients show a different trend. The lowest wear exhibits the film synthesized with a Mo target cathode power of 1 kW with a value of (1.06 ± 0.2) x10^{-5} mm^3/Nm. For a Mo target cathode power of 2 kW and the film deposited without additional Mo the wear coefficient is about 3.5 x10^{-5} mm^3/Nm and increases up to (5.93 ± 0.4) x10^{-5} mm^3/Nm for a Mo target cathode power of 3 kW. For all films, except the film deposited with a Mo target cathode power of 1 kW, the film material is completely removed from the contact area.

Considering the coefficients of friction, it is assumed that the mechanisms affecting the friction behavior change above a Mo cathode power of 1 kW. Below this value the friction is determined by the characteristics of MoS_2 and the relatively high S/Mo ratio indicates that the formation of a lubricating MoS_2 phase is possible. The beneficial effect of additional elements on the tribological behavior was also reported for Ti. Due to the Mo in the space between the S planes, respectively, in the MoS_2 lattice, the thin film is protected from oxygen contaminations and the friction is reduced (Ref 35). In addition, the formation of the (002) basal-plane and the densification of the microstructure contribute to the improved friction behavior (Ref 45). Considering the topography of the wear tracks, the coefficient of friction of the film deposited without additional Mo targets is lower in contrast to a steel - steel contact, although the film material is completely removed from the contact area. This indicates the dynamic interaction of the generated film material. The generated film particles participate during the sliding process and are just removed from the contact area after both contact partners are separated as discussed in previous investigations (Ref 20, 46). Due to the incorporation of a low amount of additional Mo, the amount of the film material contributing the lubricating effect is increased, since the breakup of the columns is complicated (Ref 47). Also, the compacted microstructure contributes to this effect (Ref 48, 49) and is reflected in a lower wear and a reduced substrate exposure for the film deposited with a Mo target cathode power of 1 kW. It is to note that there is no direct relation between the mechanical and the tribological properties. These films are characterized by a low hardness and elastic modulus as well as low H/E* and H^3/E^{*2} ratios. More important is the ability to keep the detached particles within the contact area during the sliding. This was also seen for MoS_x:N films (Ref 41) and underlines the importance of dynamic effects of the film material during the sliding process.

In contrast to that, at a further increasing Mo cathode power the friction increases. A first possible explanation is that the friction behavior is determined by the MoN phase. Although the (002) MoS_2 reflex is still present for the films deposited with a high Mo cathode power, the lubricating character of the MoS_2 phase seems to be superimposed. This could result from the decreasing amount of S in the films with an increasing Mo cathode power, since a sufficient supply of S is necessary to form lubricating phases during the tribo-test (Ref 10). This is also indicated by the low S/Mo ratio. Furthermore, for these two films, the film material is completely removed from the contact area and the substrate exposed. Therefore, it is assumed that the film material loses its ductility and is marked by a brittle character. The development of the coefficient of friction indicates that this effect occurs after a few rotations, since the coefficient of friction rises to 1 and then settles at a value of 0.7, which corresponds to a steel - steel contact (Ref 50). The sudden rise of the coefficient of friction can be justified with the breakthrough of the thin film by the counterpart due to the brittle character of the film material. Also, the Rockwell indents showed an increasing amount of cracks and delaminated film material, which is in accordance with this suggestion that the film material has a brittle character. It also supports the assumption that the MoS_2 character is completely lost. Despite, it is underlined that although the H/E* and H^3/E^{*2} ratios increase, the wear properties are impaired. This trend indicates that the mechanical properties are of minor importance for the tribological behavior due to the change of the film from a solid lubricant to a nitride.

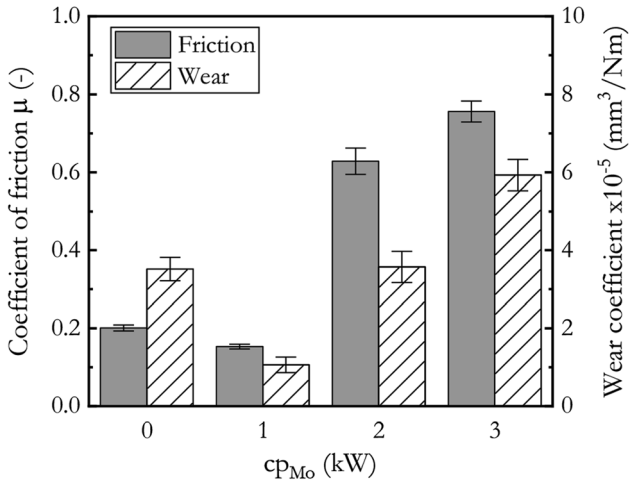

Fig. 5 Coefficients of friction and wear coefficients of the MoS_x:N:Mo thin films sliding against $100Cr_6$

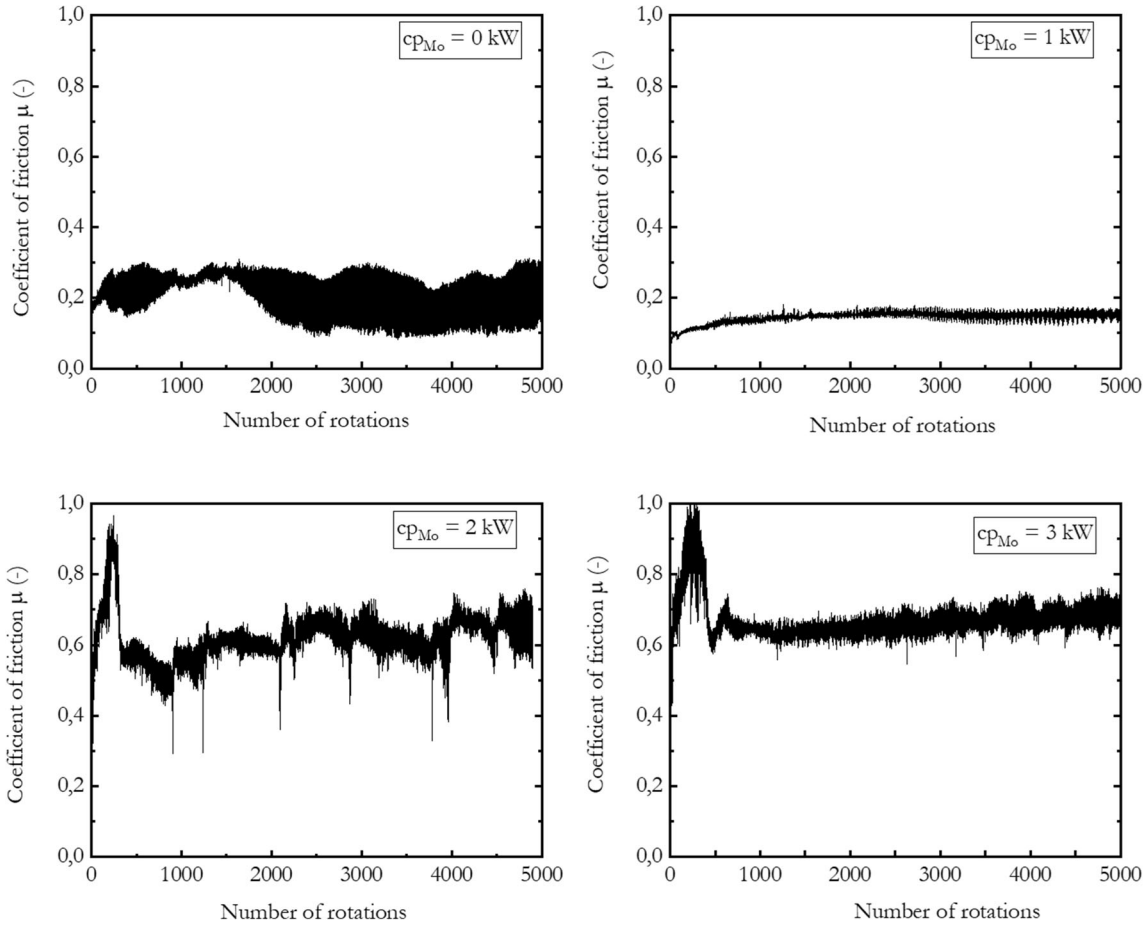

Fig. 6 Development of the coefficients of friction of the MoS_x:N:Mo thin films over the number of rotations

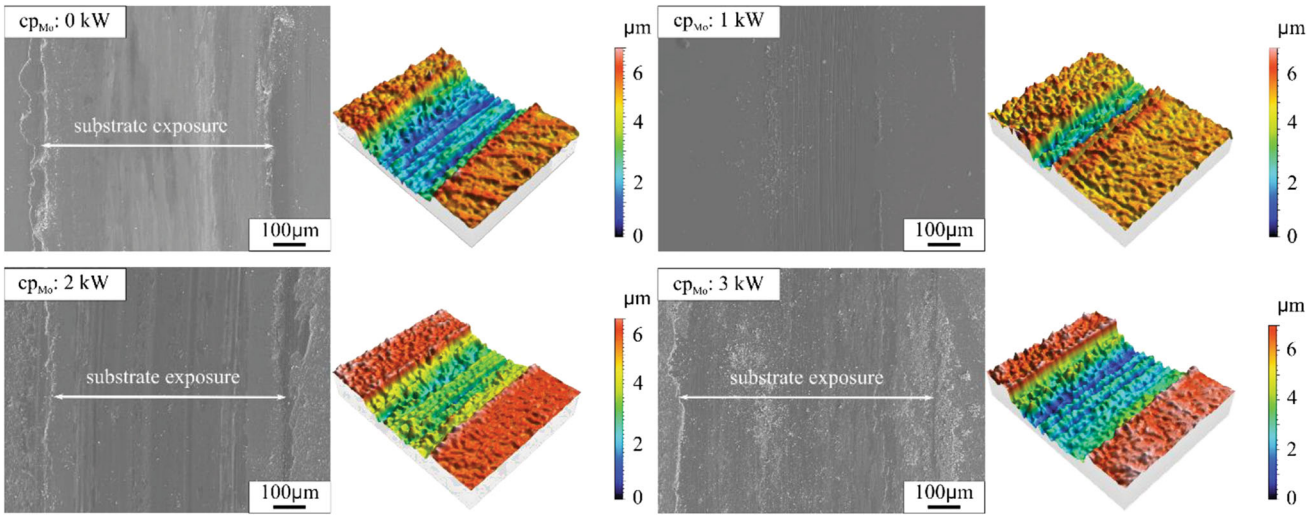

Fig. 7 SEM images and 3D-models of the wear tracks of the MoS_x:N:Mo thin films

4. Conclusion

A reactive hybrid dcMS/HiPIMS process was employed to synthesize MoS_x:N:Mo films, whereby the effect of an increasing Mo cathode power was investigated. At a low Mo cathode power, the additional Mo in the film acts as a doping element and is related to improved friction properties, which are ascribed to a densification of the microstructure and the formation of the (002) basal-plane orientation. By further increasing the Mo cathode power, the properties are determined by the formation of a MoN phase. An impaired adhesion

combined with an insufficient supply of S and Mo to form a lubricating MoS_2 phase lead to high friction and wear.

Acknowledgments

The authors gratefully acknowledge the German Research Foundation (DFG) for financially supporting this work within the priority program SPP2074 subproject "Fluid-free lubricant layers for the heavily loaded and unsynchronized operation of dry-running screw machines".

Funding

Open Access funding enabled and organized by Projekt DEAL.

Conflict of interest

The authors declared that there is no conflict of interest

References

1. A. Baptista, F. Silva, J. Porteiro, J.L. Míguez, G. Pinto and L. Fernandes, On the Physical Vapour Deposition (PVD): Evolution of Magnetron Sputtering Processes for Industrial Applications, *Procedia Manuf.*, 2018, **17**, p 746–757.
2. M.R. Vazirisereshk, A. Martini, D.A. Strubbe and M.Z. Baykara, Solid Lubrication with MoS_2, *Lubricants*, 2019, **7**, p 57.
3. T.W. Scharf and S.V. Prasad, Solid Lubricants: a Review, *J. Mater. Sci.*, 2013, **48**, p 511–531.
4. K.J. Wahl and I.L. Singer, Quantification of a Lubricant Transfer Process that Enhances the Sliding Life of a MoS_2 coating, *Tribol. Lett.*, 1995, **1**, p 59–66.
5. T. Gradt and T. Schneider, Tribological Performance of MoS_2 Coatings in Various Environments, *Lubricants*, 2016, **4**, p 32.
6. C. Donnet and A. Erdemir, Historical Developments and New Trends in Tribological and Solid Lubricant Coatings, *Surf. Coat. Technol.*, 2004, **180–181**, p 76–84.
7. N. Renevier, N. Lobiondo, V. Fox, D. Teer and J. Hampshire, Performance of MoS2/metal Composite coatings Used for Dry Machining and Other Industrial Applications, *Surf. Coat. Technol.*, 2000, **123**, p 84–91.
8. V. Fox, N. Renevier, D. Teer, J. Hampshire and V. Rigato, The Structure of Tribologically Improved MoS_2–metal Composite Coatings and Their Industrial Applications, *Surf. Coat. Technol.*, 1999, **116–119**, p 492–497.
9. X. Zhang, L. Qiao, L. Chai, J. Xu, L. Shi and P. Wang, Structural, Mechanical and Tribological Properties of Mo–S–N Solid Lubricant Films, *Surf. Coat. Technol.*, 2016, **296**, p 185–191.
10. T. Hudec, M. Mikula, L. Satrapinskyy, T. Roch, M. Truchlý, P. Švec, T. Huminiuc and T. Polcar, Structure, Mechanical and Tribological Properties of Mo-S-N Solid Lubricant Coatings, *Appl. Surf. Sci.*, 2019, **486**, p 1–14.
11. G. Strapasson, P.C. Badin, G.V. Soares, G. Machado, C.A. Figueroa, R. Hubler, A.L. Gasparin, I. Baumvol, C. Aguzzoli and E.K. Tentardini, Structure, Composition, and Mechanical Characterization of dc Sputtered TiN-MoS_2 Nanocomposite Thin Films, *Surf. Coat. Technol.*, 2011, **205**, p 3810–3815.
12. S. Gangopadhyay, R. Acharya, A.K. Chattopadhyay and S. Paul, Composition and Structure–property Relationship of Low Friction, Wear Resistant TiN–MoS_x Composite Coating Deposited by Pulsed Closed-field Unbalanced Magnetron sputtering, *Surf. Coat. Technol.*, 2009, **203**, p 1565–1572.
13. Y.W. Bae, W.Y. Lee, T.M. Besmann, C.S. Yust and P.J. Blau, Preparation and Friction Characteristics of Self-lubricating TiN-MoS_2 Composite Coatings, *Mater. Sci. Eng., A*, 1996, **209**, p 372–376.
14. X. Ding, X.T. Zeng and T. Goto, Unbalanced Magnetron Sputtered Ti–Si–N:MoS_x Composite Coatings for Improvement of Tribological Properties, *Surf. Coat. Technol.*, 2005, **198**, p 432–436.
15. R. Goller, P. Torri, M.A. Baker, R. Gilmore and W. Gissler, The Deposition of Low-friction TiN–MoS_x Hard Coatings by a Combined arc Evaporation and Magnetron Sputter Process, *Surf. Coat. Technol.*, 1999, **120–121**, p 453–457.
16. S. Carrera, O. Salas, J. Moore, A. Woolverton and E. Sutter, Performance of CrN/MoS2(Ti) Coatings for High Wear Low Friction Applications, *Surf. Coat. Technol.*, 2003, **167**, p 25–32.
17. S.K. Kim, B.C. Cha; Deposition of CrN–MoS_2 Thin Films by D.C. Magnetron Sputtering. Surf. Coat. Technol. 188-189 (2004) 174–178
18. D. Yuelan, Z. Ping, C. Zhihai et al., Effect of Mo Content on the Structural and Mechanical Properties of CrMoN/MoS_2 Composite Coatings, *Rare Metal Mater. Eng.*, 2014, **43**(2), p 264–268.
19. K. Bobzin, Synthesis, Characterization, and Tribological evaluation of HPPMS($Cr_{1-x}Al_x$)N + MoS_y Coatings, *Surf. Coat. Technol.*, 2016, **308**, p 383–393.
20. W. Tillmann, A. Wittig, D. Stangier, H. Moldenhauer, C.-A. Thomann, J. Debus, D. Aurich, A. Bruemmer, Influence of the bias-voltage, the argon Pressure and the Heating power on the Structure and the Tribological Properties of HiPIMS Sputtered MoS_x Films. Surf. Coat. Technol. (2020) 125358
21. H.E. Sliney, Solid Lubricant Materials for High Temperatures—a Review, *Tribol. Int.*, 1982, **15**, p 303–315.
22. W.C. Oliver, An Improved Technique for Determining Hardness and Elastic Modulus Using Load and Displacement Sensing, *J. Mater. Res.*, 1992, **7**, p 1564–1583.
23. S. Woo, H.C. Park and Y.-W. Son, Poisson's Ratio in Layered Two-dimensional Crystals, *Phys. Rev. B*, 2016, **93**, p 543.
24. S. Berg and I.V. Katardjiev, Preferential Sputtering Effects in Thin Film Processing, *J. Vac. Sci. Technol., A: Vac., Surf. Films*, 1999, **17**, p 1916–1925.
25. A. Aubert, J.Ph. Nabot, J. Ernoult, Ph. Renaux, Preparation and Properties of MoS_x Films Grown by d.c. Magnetron Sputtering. Surf. Coat. Technol. 41 (1990) 127–134
26. B. Vierneusel, S. Tremmel and S. Wartzack, Effects of Deposition Parameters on Hardness and Lubrication Properties of Thin MoS_2 films, *Materialwissenschaften und Werkstofftechnik*, 2012, **43**, p 1029–1035.
27. K. Sarakinos, J. Alami and S. Konstantinidis, High Power Pulsed Magnetron Sputtering: A Review on Scientific and Engineering state of the Art, *Surf. Coat. Technol.*, 2010, **204**, p 1661–1684.
28. V. Buck, Lattice Parameters of Sputtered MoS_2 films, *J. Phys. D: Appl. Phys.*, 1991, **198**, p 157–167.
29. P.D. Fleischauer, J.R. Lince, P.A. Bertrand and R. Bauer, Electronic Structure and lubrication Properties of Molybdenum Disulfide: a Qualitative Molecular Orbital Approach, *Langmuir ACS J. Surf. Coll.*, 1989, **5**, p 1009–1015.
30. M.R. Hilton, R. Bauer, S.V. Didziulis, M.T. Dugger, J.M. Keem and J. Scholhamer, Structural and Tribological Studies of MoS_2 Solid Lubricant Films Having Tailored Metal-Multilayer Nanostructures, *Surf. Coat. Technol.*, 1992, **53**, p 13–23.
31. D.G. Teer, J. Hampshire, V. Fox and V. Bellido-Gonzalez, The Tribological Properties of MoS_2/metal Composite Coatings Deposited by Closed Field Magnetron sputtering, *Surf. Coat. Technol.*, 1997, **94–95**, p 572–577.
32. G. Jayaram, L.D. Marks and M.R. Hilton, Nanostructure of Au-20% Pd Layers in MoS_2 Multilayer Solid Lubricant Films, *Surf. Coat. Technol.*, 1995, **76–77**, p 393–399.

33. H. Li, G. Zhang and L. Wang, Low Humidity-sensitivity of MoS_2/Pb Nanocomposite Coatings, *Wear*, 2016, **350–351**, p 1–9.
34. A. Nossa and A. Cavaleiro, The Influence of the Addition of C and N on the Wear Behaviour of W-S–C/N Coatings, *Surf. Coat. Technol.*, 2001, **142–144**, p 984–991.
35. N. Renevier, J. Hamphire, V. Fox, J. Witts, T. Allen and D. Teer, Advantages of Using Self-lubricating, Hard, Wear-resistant MoS_2-based Coatings, *Surf. Coat. Technol.*, 2001, **142–144**, p 67–77.
36. Z. Hui, Z. Jun, W. Qing-ping et al., The Effect of Ti content on the Structural and Mechanical Properties of MoS_2-Ti Composite Coatings Deposited by Unbalanced Magnetron Sputtering System, *Phys. Procedia*, 2011, **18**, p 234–239.
37. W. Tillmann, D. Kokalj, D. Stangier, Influence of the Deposition Parameters on the Texture and Mechanical Properties of Magnetron Sputterd Cubic MoN_x Thin Films. Materialia (2018) 100186
38. D. Depla, Chapter 5 - Sputter Deposition Processes. Handbook of Deposition Technologies for Films and Coatings (Third Edition) 7 (2010) 253–296
39. P. Barna, Fundamental Structure Forming Phenomena of Polycrystalline Films and the Structure Zone Models, *Thin Solid Films*, 1998, **317**, p 27–33.
40. P. Mutafov, M. Evaristo, A. Cavaleiro and T. Polcar, Structure, Mechanical and Tribological Properties of Self-lubricant W-S–N Coatings, *Surf. Coat. Technol.*, 2015, **261**, p 7–14.
41. W. Tillmann, A. Wittig, H. Moldenhauer, C.-A. Thomann, J. Debus, D. Aurich, A. Bruemmer, J. Nitrogen Doping of MoS_x Thin Films Sputtered by Reactive High Power Impulse Magnetron Sputtering. Thin solid films (2020) 138267
42. N. Renevier, V. Fox, D. Teer and J. Hampshire, Coating Characteristics and Tribological Properties of Sputter-deposited MoS_2/metal Composite Coatings Deposited by Closed Field Unbalanced Magnetron Sputter Ion Plating, *Surf. Coat. Technol.*, 2000, **127**, p 24–37.
43. M. Ye, G. Zhang, Y. Ba, T. Wang, X. Wang and Z. Liu, Microstructure and Tribological Properties of MoS_2+Zr Composite Coatings in High Humidity Environment, *Appl. Surf. Sci.*, 2016, **367**, p 140–146.
44. B. Deepthi, H.C. Barshilia, K.S. Rajam, M.S. Konchady, D.M. Pai and J. Sankar, Structural, Mechanical and Tribological Investigations of Sputter Deposited CrN–WS_2 Nanocomposite Solid Lubricant Coatings, *Tribol. Int.*, 2011, **44**, p 1844–1851.
45. P.D. Fleischauer, Effects of Crystallite Orientation on Environmental Stability and Lubrication Properties of Sputtered MoS_2 Thin Films, *A S L E Trans.*, 2008, **27**, p 82–88.
46. W. Tillmann, A. Wittig, D. Stangier, C.-A. Thomann, H. Moldenhauer, J. Debus, D. Aurich and A. Brümmer, Investigation of the Tribofilm Formation of HiPIMS Sputtered MoS_x Thin Films in Different Environments by Raman Scattering, *Lubricants*, 2019, **7**, p 100.
47. T. Spalvins, Structure of Sputtered Molybdenum Disulfide Films at Various Substrate Temperatures, *A S L E Trans.*, 2008, **17**, p 1–7.
48. T. Spalvins, Lubrication with Sputtered MoS2 Films: Principles, Operation, and Limitations, *JMEP*, 1992, **1**, p 347–351.
49. G. Colas, A. Saulot, E. Regis et al., Investigation of Crystalline and Amorphous MoS_2 Based Coatings: Towards Developing New Coatings for Space Applications, *Wear*, 2015, **330–331**, p 448–460.
50. I. Velkavrh, F. Ausserer, S. Klien, J. Brenner, P. Forêt, and A. Diem, The Effect of Gaseous Atmospheres on Friction and Wear of Steel–Steel Contacts Tribol. Int. 79 (2014) 99-110